Rotationally resolved spectroscopy and dynamics of the $3p_x\,{}^1A_2$ Rydberg state of formaldehyde

M. Meisinger,[a] A. M. Schulenburg,[b] F. Merkt[b] and P. P. Radi[a]

Received 12th April 2010, Accepted 15th May 2010
DOI: 10.1039/c0cp00191k

The rotational structure of the lowest three vibrational levels (0^0, 6^1 and 4^1) of the $3p_x\,{}^1A_2$ Rydberg state of formaldehyde has been studied by doubly-resonant three-photon ionization spectroscopy. A strong *a*-type Coriolis interaction between the in-plane rocking (ν_6) and out-of-plane bending (ν_4) modes results in the observation of vibronically forbidden transitions to the 6^1 level from the intermediate $\tilde{A}\,{}^1A_2$ ($2^1\,4^3$) level. The full widths at half maximum of the rovibronic transitions to the 4^1 state are considerably larger than to the vibrational ground state and the 6^1 level. The band origin (T_0 = 67 728.939(82) cm^{-1}), the rigid rotor rotational constants (A = 9.006(19) cm^{-1}, B = 1.331(20) cm^{-1}, and C = 1.135(22) cm^{-1}), the Coriolis coupling constant ($\xi^a_{4,6}$ = 8.86(89) cm^{-1}) and the deperturbed fundamental wave numbers of both vibrational modes ($\tilde{\nu}_6$ = 808.88(25) cm^{-1} and $\tilde{\nu}_4$ = 984.92(26) cm^{-1}) have been determined for the $3p_x\,{}^1A_2$ Rydberg state. Polarization effects originating from the double-resonance technique have been exploited to detect the Coriolis interaction and investigate how it affects the predissociation dynamics.

1 Introduction

Formaldehyde (H_2CO), a tetraatomic molecule with 16 electrons, is ideally suited to studies of molecular structure and dynamics by high-resolution spectroscopy and *ab initio* quantum chemistry. The structure and dynamics of the lowest two electronically excited states ($\tilde{A}\,{}^1A_2$ and $\tilde{a}\,{}^3A_2$) of H_2CO have been extensively studied[1–4] because they provide an ideal system with which to study internal conversion, intersystem crossings and their effects on the photodissociation into H_2 + CO and HCO + H.[5–10]

At higher energies a third dissociation channel (CH_2 + O) becomes accessible[11] and the density of electronically excited states increases rapidly. In the region between 60 000 and 80 000 cm^{-1} several valence states overlap with low-lying Rydberg states[12–15] and give rise to complex spectral structures.

Early studies of the absorption spectrum of formaldehyde in the vacuum ultraviolet (VUV) revealed the presence of n = 3 Rydberg states in the energy range between 7.5 and 8 eV.[16,17] The first observation of their vibrational structure was reported by Lessard and Moule, who also proposed assignments in terms of $3p_x$, $3p_y$ and $3p_z$ components.[18–20] Liu *et al.*[21] assigned several vibrational levels of the three 3p Rydberg states in studies by two-photon resonant multi-photon ionization and photoelectron spectroscopy. In parallel, self-consistent-field and configuration-interaction *ab initio* quantum chemical calculations by Peyerimhoff *et al.*[12] and Grein and coworkers[11–15] resulted in the determination of the potential energy functions of several electronically excited states of formaldehyde along the C–O stretching mode.

Of the six normal modes of formaldehyde, the out-of-plane bending mode ν_4 and the in-plane rocking mode ν_6 have the lowest frequencies. The assignment of these two vibrations in the $3p_x\,{}^1A_2$ state and in the cationic ground state has been difficult to establish unambiguously[19–22] and some uncertainty concerning the planarity/nonplanarity of the cation in its electronic ground state and the neutral molecule in the 3p Rydberg states persisted until recently.[23] In the $\tilde{X}\,{}^1A_1$ and $\tilde{A}\,{}^1A_2$ electronic states, ν_4 has a lower fundamental frequency than ν_6 , whereas the opposite holds true in the cation and the Rydberg manifold.[13,21,23]

Liu *et al.*[21] assigned two bands in the photoelectron spectrum of H_2CO to the ν_4 and the ν_6 modes of the $\tilde{X}^{+2}B_2$ ground state of the cation on the basis of the results of *ab initio* calculations[14] and determined the corresponding fundamental wave numbers to be 979 cm^{-1} and 812 cm^{-1}, respectively. They concluded that the bands observed in the (2 + 1) REMPI spectra of H_2CO at 68 542 cm^{-1} and 68 709 cm^{-1} correspond to transitions to the $3p_x\,{}^1A_2\,6^1$ and 4^1 levels, respectively, from the fact that the vibrational energy level structure of Rydberg states is similar to that of the cationic state to which the Rydberg series converges. In a rotationally resolved study of the $\tilde{X}^{+2}B_2$ ground state of H_2CO^+ by PFI-ZEKE photoelectron spectroscopy, Schulenburg *et al.*[23] then recognized that the 4^1 and 6^1 levels of the cation are subject to a Coriolis interaction.

We report here on a new investigation of the structure and dynamics of the $3p_x\,{}^1A_2$ state of H_2CO following $(1+1'+1^{(\prime)})$ doubly-resonant three-photon ionization from the ground state *via* selected rotational levels of the $\tilde{A}\,{}^1A_2$ ($2^1 4^3$) and ($2^2 4^1$) intermediate levels. Thanks to the selectivity and polarization dependence of this excitation sequence, the rotational structure of the $3p_x\,{}^1A_2$ Rydberg state could be resolved, a Coriolis interaction between the 4^1 and the 6^1 levels identified and its effect on the dissociation dynamics investigated.

[a] *Department of General Energy, Paul Scherrer Institute, CH-5232 Villigen, Switzerland*
[b] *Laboratorium für Physikalische Chemie, ETH Zürich, CH-8093 Zürich, Switzerland*

2 Experimental

The experiment is based on a $(1+1'+1^{(\prime)})$ doubly-resonant three-photon ionization scheme applied to an internally cold sample of formaldehyde in a pulsed supersonic beam. A selected rotational state $J'_{K'_aK'_c}$ in the $\tilde{A}\,^1A_2$ (2^14^3) or (2^24^1) states is populated by excitation from a rotational level $J''_{K''_aK''_c}$ of the $\tilde{X}\,^1A_1$ ground electronic state using UV radiation of wave number $\tilde{\nu}_1 \approx 30\,340$ cm^{-1} (Here and below, the rotational quantum numbers of the $\tilde{X}\,^1A_1$ ground electronic state are labeled $J''_{K''_aK''_c}$, and those of the $\tilde{A}\,^1A_2$ intermediate and $3p_x\,^1A_2$ final states $J'_{K'_aK'_c}$ and J_{K_a,K_c}, respectively). UV light in the range of 37 000–38 500 cm^{-1} ($\tilde{\nu}_2$) is then used to excite the molecules to the $3p_x\,^1A_2$ Rydberg state, and the molecules are ionized following absorption of a third photon of wave number $\tilde{\nu}_1$ or $\tilde{\nu}_2$.

The cold molecular beam is generated in a supersonic expansion of formaldehyde through a pulsed valve mounted on an *xyz*-translation stage. The source holder is resistively heated by two separate heating loops (Thermocoax). H_2CO is produced by heating a sample of *para*-formaldehyde, a solid polymer, to $\approx$350 K to liberate the monomer[24] which is subsequently co-expanded with krypton. The valve[25] is operated at a stagnation pressure in the range between 0.5 to 3 bar at a repetition rate of $16\frac{2}{3}$ Hz. The gas pulses typically have a duration of $\approx$200 μs. The rotational temperature of H_2CO in the supersonic beam is estimated to be $\approx$15 K, as determined from the line intensities of a $(1+2)$ REMPI spectrum of the $2^1_04^3_0$ band of the $\tilde{A}\,^1A_2 - \tilde{X}\,^1A_1$ transition. Because *para* and *ortho* nuclear spin isomers do not interconvert in the supersonic expansion both $K''_a = 0$ and $K''_a = 1$ rotational levels are significantly populated.[26]

The experimental multiphoton ionization setup has been described in ref. 27. Two tunable dye lasers (Lambda Physik, Scanmate and ScanMate Pro, utilizing DCM and Coumarin 153 dyes), pumped at a repetition rate of $16\frac{2}{3}$ Hz by the second and third harmonic of a pulsed Nd-YAG laser (Quantel YG 981 E) are used to selectively excite single rovibronic transitions in both excitation steps. The outputs of the dye lasers at $\approx$660 nm and $\approx$534 nm are frequency-doubled with β-barium borate (BBO) crystals. The laser beams are then overlapped using a dichroic mirror and guided collinearly into the vacuum chamber where they intersect the molecular beam at right angles. The ions produced by multiphoton ionization are subsequently accelerated in the direction perpendicular to both the molecular beam and the laser beams by an electric field of 400 V cm^{-1}, generated by applying pulsed voltages to a set of six equally spaced cylindrical extraction plates housed in two concentric mu-metal cylinders. The ions are detected by a microchannel plate (MCP) detector at the end of a flight tube.

A digital oscilloscope and a PC are used to acquire and store the data for further processing. A typical signal is averaged over 10–20 experimental cycles at each scan step ($\approx$0.14 cm^{-1} increment). For absolute calibration, a wavelength meter (High Finesse/Angstrom WS6) with an accuracy of $\approx$0.03 cm^{-1} is employed. In addition, optogalvanic spectra of Ne and Fe are recorded simultaneously with the multiphoton ionization spectra to validate the absolute wavelength calibration of the wavelength meter.

3 Results and discussion

3.1 The vibrational ground state of the $3p_x$ Rydberg state

An overview of the doubly-resonant three-photon ionization spectra of formaldehyde obtained by selecting different rotational levels of the $\tilde{A}\,^1A_2$ ($2^1\,4^3$) state with the first laser and scanning the wave number of the second laser in the region of the $3p_x\,^1A_2 - \tilde{A}\,^1A_2\,2^0_14^0_3$ band is displayed in Fig. 1. All spectra have been shifted along the wave-number axis so that the line positions correspond to the absolute energies of the rotational levels of the $3p_x\,^1A_2$ state above the lowest rovibrational level of the $\tilde{X}\,^1A_1$ ground state. The selectivity of the doubly-resonant excitation scheme reduces the spectral congestion and facilitates the assignments which are indicated by the asymmetric-top rotational quantum numbers $J_{K_aK_c}$ of the $3p_x\,^1A_2$ state above the assignment bars. The rotational quantum numbers $J'_{K'_aK'_c}$ of the selected level of the $\tilde{A}\,^1A_2$ state are given on the left-hand side of the corresponding traces. The full widths at half maximum (FWHM) of the observed lines are larger (1.2 cm^{-1}) than the laser bandwidths ($\approx$0.2 cm^{-1}) and the lineshapes are well described by Lorentzian functions which suggest that they reflect the predissociation lifetime of the ground vibrational level of the $3p_x\,^1A_2$ state.

The transition wave numbers obtained by fitting Lorentzian lineshape functions to the experimental lineshapes are summarized in Table 1 and were used to determine the spectroscopic parameters (rotational constants and band origin) in a nonlinear least-squares fitting procedure using the software package pgopher.[28] The rotational constants of the $\tilde{A}\,^1A_2$ ($2^1\,4^3$) level were kept fixed at their known values.[3] The results of the fit are presented in Table 2 where they are compared with the results of ref. 21, 23. Because of the low temperature of the H_2CO sample, only $J \leq 4$ rotational levels of the $3p_x\,^1A_2$ state could be accessed, and a rigid-rotor Hamiltonian turned out to be adequate to describe the experimental line positions. The average error of the fit, $\sum_i (\delta\tilde{\nu}_i)^2/(n_{\mathrm{obs}} - n_{\mathrm{par}})$, with $n_{\mathrm{obs}} = 30$ observed values and $n_{\mathrm{par}} = 4$ adjustable parameters, is indeed 0.22 cm^{-1} with a maximum deviation of 0.52 cm^{-1} for the $^rQ_{11}(2)$ transition. This particularly large deviation originates from the fact that the $^rQ_{11}(2)$ line forms a shoulder on the side of the much stronger $^rR_{10}(1)$ transition.

The term value of the $3p_x\,^1A_2$ state determined in the fit ($T_0 = 67\,728.939(82)$ cm^{-1}) is in good agreement with that determined earlier by Liu *et al.*,[21] and the rigid-rotor rotational constants B and C lie close to the values determined for the cationic ground state.[23] The decrease of the A rigid-rotor constant suggests that the HCH angle increases upon ionization. Our analysis supports the conclusion drawn by Liu *et al.*[21] that the observed band is not, as suggested earlier by Mentall *et al.*,[22] a doublet band resulting from an inversion manifold caused by a nonplanar geometry. Instead, the structure stems from the K_a substructure that could be partially resolved in ref. 21 leading to an estimation of the rotational constant A of 9 cm^{-1}. The inertial defect of the $3p_x\,^1A_2$ state, $\Delta = I_c - I_b - I_a$ is 0.315(94) amuA^2, where I_i ($i = a, b, c$) denote the principal moments of inertia, and also suggests a planar structure.[29,30]

To calculate the relative intensities in double-resonance spectra, the alignment effects caused by the coherent

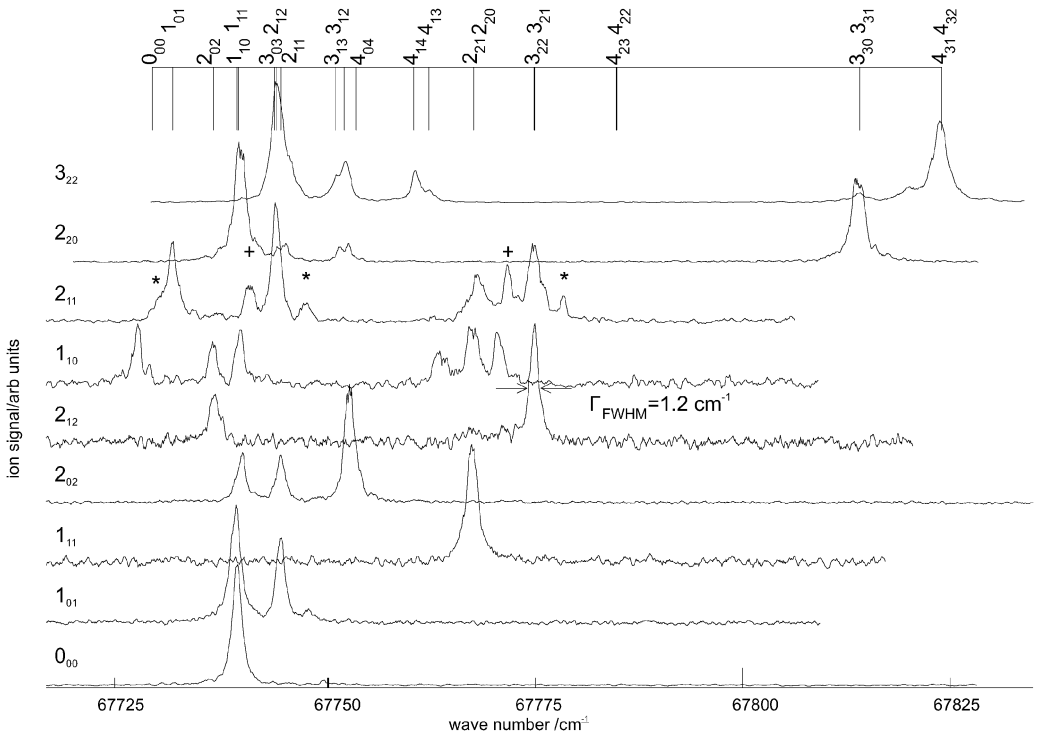

Fig. 1 Overview of the doubly-resonant three-photon ionization spectra of the $3p_x\,^1A_2\ 0^0$ state of H_2CO. The x-axis indicates the total wave number above the $\tilde{X}^1A_1\ (0^0)\ 0_{00}$ rovibronic ground state of H_2CO. The selected intermediate rotational levels ($J'_{K'_aK'_c}$) of the $\tilde{A}\,^1A_2\ (2^14^3)$ state are indicated on the left-hand side. The labels above the assignment bar indicate the rotational levels of the $3p_x\,^1A_2$ state. The transitions marked with asterisks and pluses arise from the levels $\tilde{A}\,^1A_2\ (2^14^3)\ 3_{12}$ and 1_{10}, which are populated simultaneously with the $J'_{K'_aK'_c} = 2_{11}$ level because of overlapping transitions in the first excitation step.

interaction of the molecules with the laser fields must be considered.[31] The relative line strength of a transition is proportional to a purely geometric factor accounting for the polarization dependence of a doubly-resonant two-photon absorption process,

$$S = \sum_{M,M''} \begin{pmatrix} J'' & 1 & J' \\ -M'' & -S_2 & M' \end{pmatrix}^2 \begin{pmatrix} J' & 1 & J \\ -M' & -S_1 & M \end{pmatrix}^2, \quad (1)$$

where M'', M', and M designate the magnetic sublevels of the ground, intermediate and excited states, respectively, and S_1 and S_2 are 0 if both excitation fields are polarized in z-direction.

Four rotationally resolved spectra of the $3p_x\,^1A_2$ ground vibrational level are presented in panels (a)–(d) of Fig. 2, corresponding to the excitation sequences (a) $1_{10} \rightarrow 1_{01} \rightarrow 3p_x$, (b) $1_{11} \rightarrow (2_{20},2_{21}) \rightarrow 3p_x$, (c) $1_{10} \rightarrow 2_{12} \rightarrow 3p_x$ and (d) $1_{01} \rightarrow 1_{10} \rightarrow 3p_x$ and $2_{02} \rightarrow 2_{11} \rightarrow 3p_x$. For comparison, spectra calculated using eqn (1) and the molecular constants determined in the least-squares fit are displayed as dotted lines. Overall, the agreement between measured and calculated spectra is good with two exceptions: the measured intensity of the unresolved transitions to the $3p_x\ 3_{31}$ and 3_{30} levels in panel (b) are smaller than predicted by the calculations, and, in panel (d), the measured intensities of the transition to the $3p_x\ K_a = 0$ levels are stronger than the calculated ones. This latter difference could be caused by a preferential excitation of the 2_{11} intermediate level in the first excitation step. Deviations between calculated and measured intensities may also result from the predissociation dynamics of the intermediate states selected in the multiphoton ionization sequence. The calculations of polarization-dependent line strength factors (eqn (1)) accounts for the absence of the transition to the $3p_x\ 0_{00}$ level in panel (d) for the case $S_1 = S_2 = 0$.

The dependence of the relative intensities on the initial excitation step is illustrated by Fig. 3 which compares, in panel (a), the excitation to $3p_x\,^1A_2$ from $J'_{K'_aK'_c} = 2_{02}$, which is excited from $J''_{K''_aK''_c} = 1_{11}$ (upper trace) and 2_{11} (lower trace) and, in panel (b), spectra obtained through $J'_{K'_aK'_c} = 1_{11}$ excited from the 0_{00} (upper trace) and 2_{02} (lower trace) ground state levels. Although the relative intensities within each pair of spectra differ substantially, they are nicely accounted for by the calculations for $S_1 = S_2 = 0$ (dotted lines). The absence of the transitions to the $3p_x\ 1_{01}$ level in the upper trace of panel (b) and to the $3p_x\ 0_{00}$ level in Fig. 2d illustrates the good experimental control of the relative polarization of the two lasers.

The $3p_x\ 0_{00}$ level would be observable from the intermediate 1_{10} level in the same ($S_1 = S_2 = 0$) polarization configuration but from the $J''_{K''_aK''_c} = 2_{20}$ ground state level. However, this level is not significantly populated in the cold supersonic expansion. An alternative way of observing this level is to modify the relative polarization of the two lasers, as demonstrated in Fig. 4, the upper (lower) trace of which was recorded at a 54.7° "magic" angle (at the angle 0°) between the two polarization vectors *via* the $\tilde{A}\,2^14^3\ 1_{10}$ intermediate level.

Table 1 Observed wave numbers of the rotationally resolved $2^0_1 4^0_3$ and $2^0_2 4^0_1$ bands of the $3p_x\,{}^1A_2$–$\tilde{A}\,{}^1A_2$ transition of H_2CO. The lines are assigned using the notation ${}^{\Delta K_a}\Delta J_{K'_a K'_c}(J')$. The deviations of the calculated from the observed values $\delta\tilde{\nu} = \tilde{\nu}_{obs} - \tilde{\nu}_{calc}$ are listed in the second column. The root-mean-square deviation of the fit is 0.22 cm^{-1}

${}^{\Delta K_a}\Delta J'_{K'_a K'_c}(J')$	$\tilde{\nu}_{obs}$	$\delta\tilde{\nu}$
${}^rR_{10}(1)^a$	37 068.10	0.13
${}^pP_{10}(1)^a$	37 060.49	−0.15
${}^pP_{11}(2)^a$	37 071.20	0.20
${}^pR_{11}(2)^a$	37 058.83	0.04
${}^pR_{11}(1)^a$	37 071.27	0.27
${}^rQ_{11}(2)^a$	37 095.36	0.52
${}^rR_{10}(1)^a$	37 099.17	0.03
${}^pR_{10}(1)^a$	37 068.16	0.19
${}^rR_{00}(0)$	37 399.29	0.05
${}^rQ_{01}(1)$	37 396.71	−0.21
${}^rR_{01}(1)$	37 402.15	−0.07
${}^rR_{11}(1)$	37 418.10	−0.07
${}^rR_{10}(1)$	37 417.79	−0.29
${}^pR_{10}(1)$	37 386.52	−0.40
${}^rR_{11}(2)$	37 420.82	−0.28
${}^rQ_{11}(2)$	37 413.69	−0.06
${}^rQ_{12}(3)$	37 414.59	−0.01
${}^pP_{11}(2)$	37 377.47	−0.23
${}^pR_{11}(2)$	37 389.82	−0.08
${}^rR_{02}(2)$	37 405.87	0.25
${}^rP_{02}(2)$	37 393.09	0.20
${}^rQ_{02}(2)$	37 397.84	0.47
${}^pQ_{12}(2)$	37 382.83	−0.04
${}^rR_{12}(2)$	37 421.44	0.07
${}^rR_{20}(2)$	37 438.71	0.03
${}^pP_{20}(2)$	37 364.19	−0.04
${}^pQ_{20}(2)$	37 368.80	0.08
${}^pR_{20}(2)$	37 377.07	0.10
${}^pQ_{21}(2)$	37 369.49	0.16
${}^pR_{21}(2)$	37 375.90	0.16

[a] Transitions from $\tilde{A}\,{}^1A_2\ 2^2 4^1$.

Table 2 Rigid-rotor asymmetric-top rotational constants, band origin T_0, Coriolis constant $\xi^a_{4,6}$ and fundamental wave numbers of the out-of-plane bending (ν_4) and in-plane rocking (ν_6) modes of the $3p_x\,{}^1A_2$ state of H_2CO derived from the experimental spectra in a least-squares fit. The values in parenthesis represent one standard deviation in units of the last digit. The uncertainty in the value of the band origin does not include a systematic uncertainty of 0.5 cm^{-1}

	This work	Ref. 23 and 21*
A/cm^{-1}	9.006(19)	8.874(8)
B/cm^{-1}	1.331(20)	1.342(15)
C/cm^{-1}	1.135(22)	1.148(18)
T_0/cm^{-1}	67 728.939(82)	67 730(2)*
$\tilde{\nu}_6/cm^{-1}$	808.88(25)	812*
$\tilde{\nu}_4/cm^{-1}$	984.92(26)	979*
$\xi^a_{4,6}/cm^{-1}$	8.86(89)	8.70(10)

3.2 Coriolis interaction of the 6^1 and the 4^1 levels

As mentioned in the introduction, Liu *et al.*[21] observed two vibrational bands at approximately 800 cm^{-1} and 1000 cm^{-1} above the origin of the $3p_x$ state by nonresonant two-photon excitation from the ground state and assigned them to the 6^1 and the 4^1 levels of the $3p_x\,{}^1A_2$ state, respectively.

In the present investigation, doubly-resonant three-photon ionization spectra were recorded in the same spectral region *via* the $\tilde{A}\,2^1 4^3$ level. Because the transition from the $\tilde{A}\,2^1 4^3$ to the $3p_x\,6^1$ level is vibronically forbidden, we originally hoped that the doubly-resonant spectra would only consist of one band corresponding to the transition to the $3p_x\ 4^1$ level, and thus provide a straightforward and unambiguous assignment of the 4^1 and 6^1 levels. However, contrary to our expectation, our spectra, displayed in Fig. 5, consist of two vibrational bands, one centered around 68 550 cm^{-1}, the other around 68 720 cm^{-1}. To clarify the assignment and understand the reason for the observation of the 6^1 level of the $3p_x$ state, spectra were recorded through the selected $J'_{K'_a K'_c} = 2_{20/1}$, 2_{02}, $3_{21/2}$, 1_{11}, and 2_{11} levels of the $\tilde{A}\,{}^1A_2$ ($2^1 4^3$) state, as depicted in Fig. 5. The two vibrational bands display an identical parallel band structure with $\Delta K_a = 0$, which can be recognized by superimposing the rotational structure of both bands recorded from the same intermediate state $J'_{K'_a K'_c}$ (see Fig. 6). Assuming equal selection rules for the two observed bands, and analyzing the rotational structure of each band separately using the same rigid-rotor model as used for the ground vibrational state of the $3p_x$ level, led to the following set of molecular constants: $\tilde{\nu}_i = 809.5\ cm^{-1}$, $A_i = 8.62\ cm^{-1}$, $B_i = 1.34\ cm^{-1}$, and $C_i = 1.14\ cm^{-1}$ for the lower level, and $\tilde{\nu}_j = 985.6\ cm^{-1}$, $A_j = 9.52\ cm^{-1}$, $B_j = 1.36\ cm^{-1}$, and $C_j = 1.16\ cm^{-1}$ for the upper vibrational levels. Whereas the values of the B and C rotational constants are identical, within the experimental uncertainties, to those of the ground state, the A constants differ markedly and indicate a perturbation.

A striking aspect of the spectra depicted in Fig. 5 and 6 concerns the very different linewidths. Whereas the transitions to the lower vibrational level have a Lorentzian line shape with full width at half maximum $\Gamma_{FWHM,i} \approx 2.5\ cm^{-1}$ (which corresponds to a lifetime of ≈ 2 ps) and are well resolved, the transitions to the upper vibrational level are much broader ($\Gamma_{FWHM,j} \approx 11\ cm^{-1}$, corresponding to a lifetime of ≈ 0.5 ps) and partially overlap.

A detailed consideration of the spectra depicted in Fig. 5 reveals anomalies which point at a large Coriolis interaction along the a axis which couples the 4^1 and 6^1 vibrational levels. Firstly, the lower vibrational level is not observed in the spectrum recorded from the $J'_{K'_a K'_c} = 2_{02}$ intermediate level. The selection rule $\Delta K_a = 0$ for a parallel transition restricts, in this case, the excitation to $K_a = 0$ levels which are not affected by a Coriolis interaction along the a axis. This observation leads to the conclusion that the mechanism by which the transition to the lower vibrational level gains its intensity *must be* an a-type Coriolis interaction. Consequently, the lower of the two vibrational bands can be assigned to the vibronically forbidden transition to the 6^1 vibrational level, and the upper band to a transition to the vibronically allowed 4^1 level, thus proving the vibrational assignments proposed by Liu *et al.*[21]

Secondly, a strong a-type Coriolis interaction also accounts for the large differences in A constants obtained in the rigid-rotor fits discussed above. An a-type Coriolis interaction causes a strong local perturbation of the rigid-rotor energy level structure if the K-manifolds overlap. However, if the vibrational states are well separated energetically, as is the case here, the main effects of a strong a-type Coriolis interaction are to increase the separation between the two bands and to modify the A constants significantly: for the energetically lower-(higher-)lying vibrational level, the A constant is

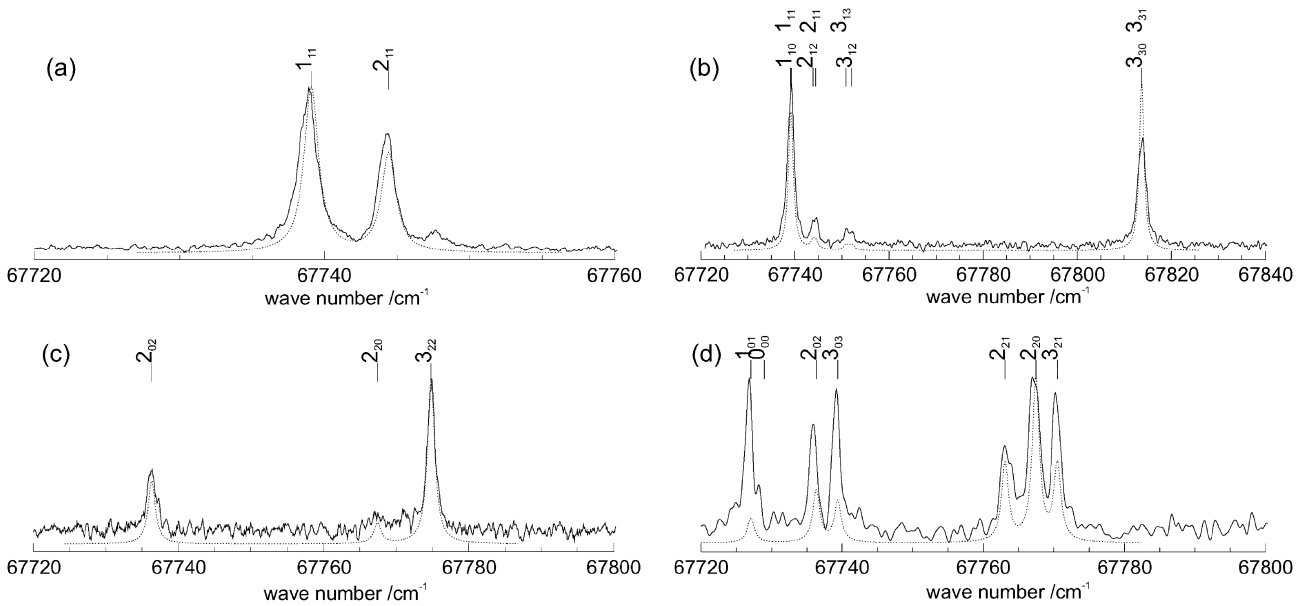

Fig. 2 Comparison of experimental and calculated spectra of transitions from selected rotational levels ($J'_{K'_aK'_c}$) of the intermediate $\tilde{A}\,{}^1A_2$ (2^14^3) state to the vibrational ground level of the $3p_x\,{}^1A_2$ Rydberg state of H_2CO. (a) $J'_{K'_aK'_c} = 1_{01}$ excited from the ground neutral state with the ${}^pQ_{10}(1)$ transition (using the notation ${}^{\Delta K_a}\Delta J_{K''_aK''_c}(J'')$). (b) $J'_{K'_aK'_c} = 2_{20}$ and 2_{21} excited at the position of the overlapping ${}^rR_{11}(1)$ and ${}^rR_{10}(1)$ transitions of the $2^1_04^3_0$ band. (c) $J'_{K'_aK'_c} = 2_{12}$ excited with the ${}^rR_{11}(1)$ transition. (d) $J'_{K'_aK'_c} = 1_{10}$ and 2_{11} excited at the position of the overlapping ${}^rQ_{01}(1)$ and ${}^rQ_{02}(2)$ transitions of the $2^1_04^3_0$ band.

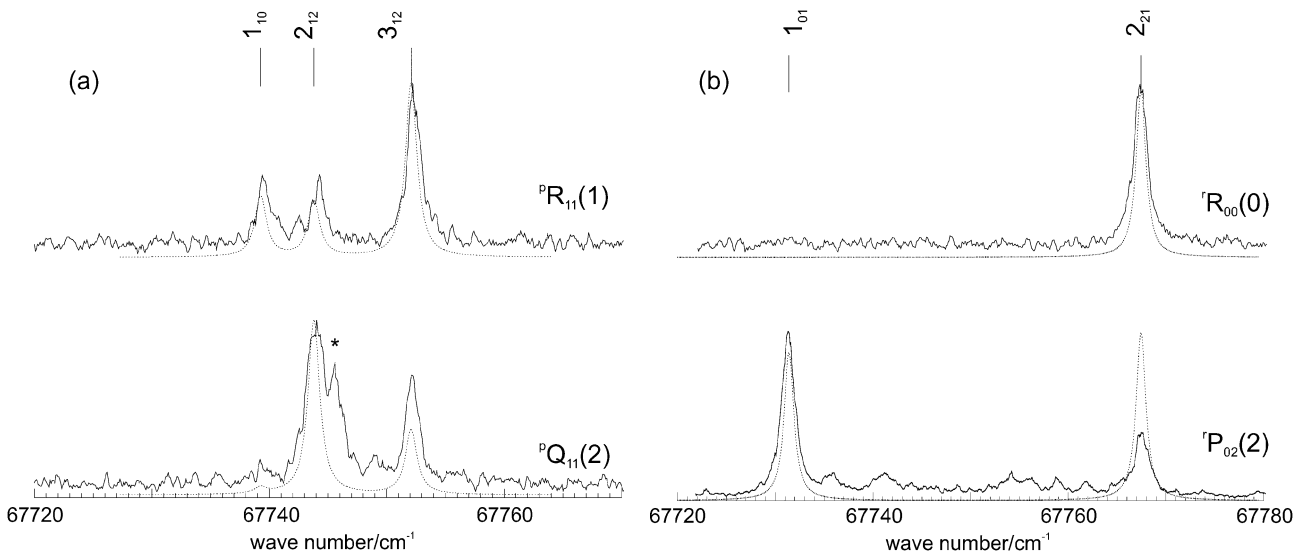

Fig. 3 Dependence of the doubly-resonant three-photon ionization spectra of H_2CO on the transitions used to prepare the $J'_{K'_aK'_c}$ rotational level of the $\tilde{A}\,{}^1A_2$ (2^14^3) state. The two panels show spectra obtained from the intermediate states $J'_{K'_aK'_c} = 2_{02}$ (a) and 1_{11} (b). (a) The 2_{02} state is excited from $J''_{K''_aK''_c} = 1_{11}$ (upper trace) and 2_{11} (lower trace). The transition marked with an asterisk arises from the transition to $J_{K_aK_c} = 1_{11}$ from $J'_{K'_aK'_c} = 0_{00}$, which is excited simultaneously with the ${}^pQ_{11}(2)$ transition in the first excitation step, and is not considered in the simulation. (b) The 1_{11} level is excited from $J''_{K''_aK''_c} = 0_{00}$ (upper trace) and 2_{02} (lower trace).

reduced (becomes larger), in qualitative agreement with the values of the fitted effective rotational constants listed above.

Finally, an *a*-type Coriolis interaction also enables one to rationalize, to some extent, the ratios of linewidths and intensities observed for the two bands, as shall be discussed in more detail at the end of this subsection.

Coriolis coupling between the 4^1 and the 6^1 vibrational states is a well-understood characteristic of the $\tilde{X}\,{}^1A_1$ electronic ground state of neutral formaldehyde. Recently, we have reported and analyzed a strong *a*-type Coriolis interaction between the 4^1 and 6^1 vibrational levels of the $\tilde{X}^+$ electronic ground state of the formaldehyde cation.[23] Given that the rovibrational structure of Rydberg states closely resemble that of the cationic state to which the Rydberg series converge, the existence of a similar interaction in the $3p_x$ level of H_2CO and in the ground state of H_2CO^+ is not surprising.

To account for the Coriolis coupling, the same procedure was followed as in our study of the cationic ground state.[23]

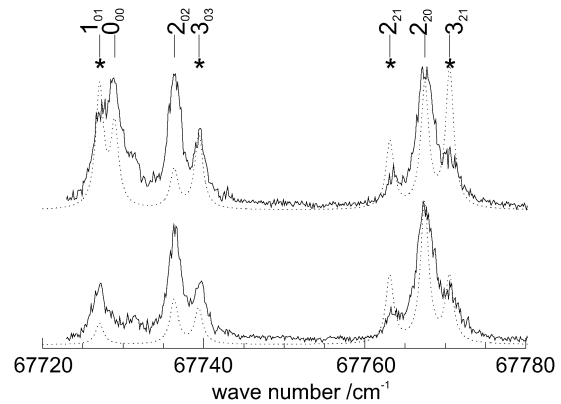

Fig. 4 Doubly-resonant three-photon ionization spectra of H_2CO recorded *via* the intermediate $\tilde{A}\,^1A_2$ (2^14^3) $J'_{K'_aK'_c} = 1_{10}$ and 2_{11} levels populated by overlapping transitions recorded with parallel polarization (lower trace) and at an angle of 54.7 degrees between the two electric field vectors (upper trace). Calculated spectra (dotted lines) are displayed for comparison. The peaks marked with asterisks are transitions originating from excitation from the $J'_{K'_aK'_c} = 2_{11}$ intermediate level.

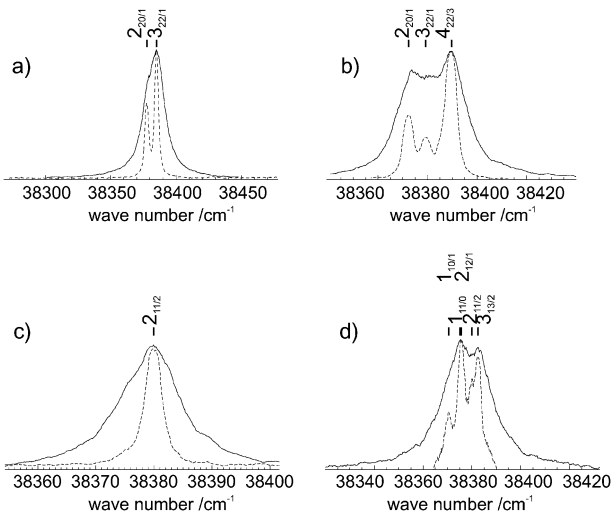

Fig. 6 Parallel band structure of the transitions from the $\tilde{A}\,^1A_2$ (2^14^3) intermediate state to the 4^1 and 6^1 levels of the $3p_x\,^1A_2$ state of H_2CO. The spectra of the transitions to the 6^1 level (thin dashed traces) are shifted along the horizontal axis to demonstrate that the same selection rule $\Delta K_a = 0$ holds for both vibronic transitions. The excitation was performed *via* the intermediate states (a) $J'_{K'_aK'_c} = 2_{20}$ and 2_{21}, (b) $J'_{K'_aK'_c} = 3_{12}$ and 3_{13}, (c) $J'_{K'_aK'_c} = 1_{11}$, and (d) $J'_{K'_aK'_c} = 1_{10}$ and 2_{11}.

The rigid-rotor Hamiltonian $H_{RR} = \hbar^{-2}\,(A\hat{J}_z^2 + B\hat{J}_x^2 + C\hat{J}_y^2)$ was extended by the term

$$V_{Cor} = A\zeta^a_{4,6}(Q_4\hat{P}_6 - Q_6\hat{P}_4)\hat{J}_a, \qquad (2)$$

where Q_i represents the i-th normal coordinate ($i = 4$ or 6), $\hat{P}_i$ the i-th conjugate momentum and $\zeta^a_{4,6}$ the Coriolis coupling constant as defined in ref. 32. In the basis of symmetric-top wave functions $|J, K, v_4, v_6\rangle$, the Hamiltonian possesses off-diagonal matrix elements proportional to $\zeta^a_{4,6}\cdot K$ for pairs

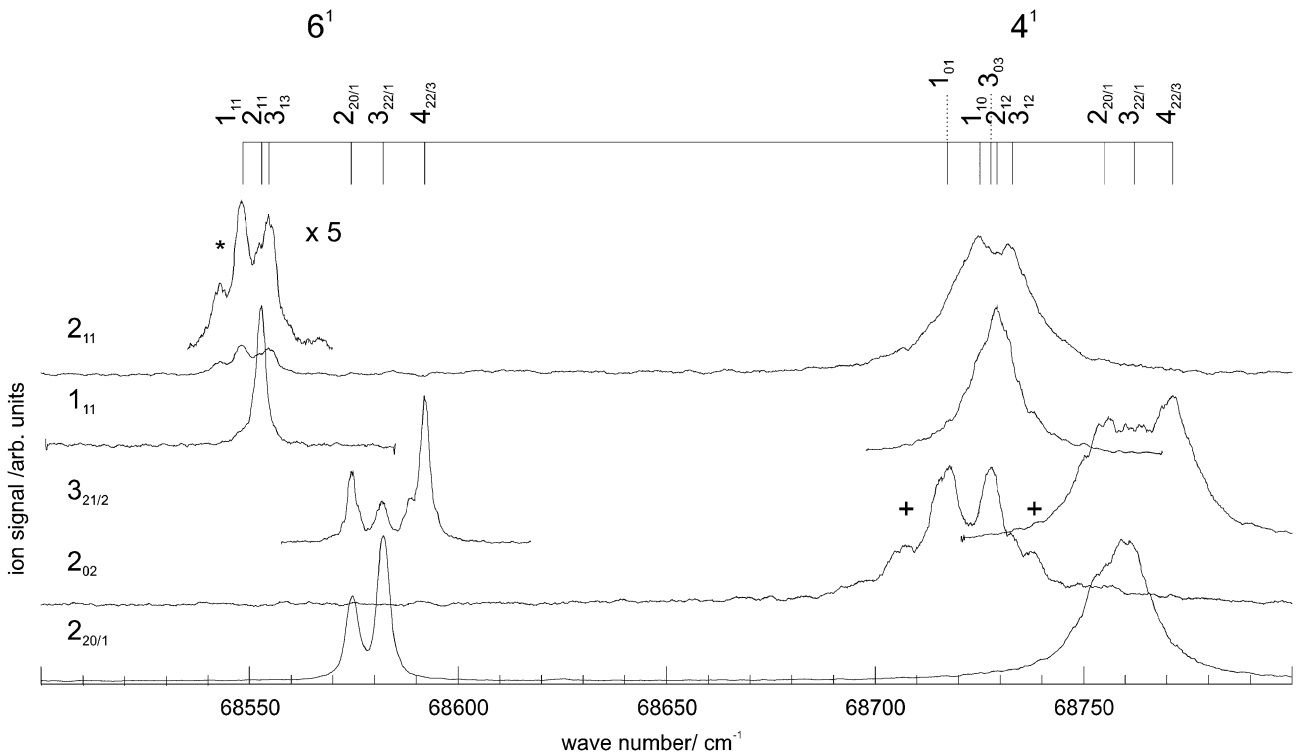

Fig. 5 Doubly-resonant three-photon ionization spectra of the $3p_x\,^1A_2$ 6^1 and 4^1 levels of H_2CO recorded *via* selected rotational levels of the $\tilde{A}\,^1A_2$ (2^14^3) state as indicated on the left-hand side of each trace. The lines on the high-wave-number side correspond to transitions to the 4^1 state and exhibit an *a*-type structure. The narrow lines on the low-wave-number side are vibronically forbidden transitions to the 6^1 state which are observed as a result of Coriolis coupling with the 4^1 state. The transition marked with the asterisk arises from excitation from $J'_{K'_aK'_c} = 1_{10}$ and those marked with a plus from $J'_{K'_aK'_c} = 3_{03}$. These intermediate levels are simultaneously populated by close-lying transitions to the $\tilde{A}\,^1A_2$ (2^14^3) state.

of wave functions in the 4^1 and the 6^1 states with equal J and K values, where

$$\xi^a_{4,6} = A\zeta^a_{4,6}\left(\sqrt{\frac{\tilde{\nu}_6}{\tilde{\nu}_4}} + \sqrt{\frac{\tilde{\nu}_4}{\tilde{\nu}_6}}\right), \qquad (3)$$

as defined in ref. 33. Consequently, asymmetric-top rotational levels with equal values of J and K_a, and K_c values differing by 1, are coupled, because only levels with equal rovibronic symmetry can interact. These selection rules were already used above to assign the vibrational levels on the basis of the nonobservation of the 6^1 level in the spectrum recorded from the $J'_{K'_aK'_c} = 2_{02}$ intermediate level (see Fig. 5).

The limited number of observed transitions prevented a global fit including the deperturbed rotational constants A, B and C, the Coriolis coupling constant $\xi^a_{4,6}$ and the fundamental wave numbers of the ν_4 and ν_6 modes. Instead, the rotational constants A, B and C were kept fixed at the rigid-rotor values derived for the $3p_x\ ^1A_2$ vibrational ground state, and only the vibrational term values and the Coriolis coupling constant were adjusted. The results of the least-squares fit are presented in the lower part of Table 2. The deperturbed values obtained for the fundamental wave numbers of the two vibrational modes are $\tilde{\nu}_6 = 808.88(25)\ cm^{-1}$ and $\tilde{\nu}_4 = 984.92(26)\ cm^{-1}$. The value of $8.86(89)\ cm^{-1}$ of the Coriolis coupling constant is comparable to that of the electronic ground state of the neutral ($10.414368(140)\ cm^{-1}$ [3]) and the ion ($8.70\ cm^{-1}$ [23]). The wave numbers of the lines (labeled in the notation $^{\Delta K_a}\Delta J_{K'_aK'_c}(J')$) of the $2^0_1 4^0_3 6^1_0$ and the $2^0_1 4^1_3$ bands of the $3p_x\ ^1A_2$–$\tilde{A}\ ^1A_2$ transition are listed in Table 3 where the deviations between observed and calculated positions are also given. In some cases, several lines of the $2^0_1 4^1_3$ band formed unresolved clusters which prevented the determination of the line centers. The root-mean-square deviation of the fit is 0.44 cm^{-1}, which can be considered excellent given the large width of $\approx 11\ cm^{-1}$ (FWHM) of the transitions of the $2^0_1 4^1_3$ band. The largest deviations are $0.42\ cm^{-1}$ for the $2^0_1 4^0_3 6^1_0$ band and $0.89\ cm^{-1}$ for the $2^0_1 4^1_3$ band.

Polarization effects, as described above for the vibrational ground state, are also observable in the spectra of the vibrationally excited states, as illustrated by Fig. 7. These spectra were obtained using the sequences $0_{00} \rightarrow 1_{11} \rightarrow 3p_x$ (upper trace) and $2_{02} \rightarrow 1_{11} \rightarrow 3p_x$ (lower trace). In the former case, the transition to the $3p_x\ 6^1\ 1_{11}$ level is missing, and so is the transition to the $3p_x\ 4^1\ 1_{10}$ level because expression (1) yields zero for an R transition from $J'' = 0$ followed by a Q transition, when $S_1 = S_2 = 0$. In the latter case, both transitions are observable according to expression (1), and also observed, in agreement with the calculated spectra presented as dotted lines in the figure.

The simple Coriolis model presented above enables a qualitative discussion of the relative intensities and linewidths of the observed transitions. Given that the intensity of the transition to the 6^1 level is entirely "borrowed" from the transition to the 4^1 level (see discussion of Fig. 5), one may expect that it should be proportional to the 4^1 character of the eigenstates. The wave functions of the coupled rovibronic levels are linear combinations of the uncoupled symmetric-top wavefunctions $|J, K, v_4, v_6\rangle$. In the case of the coupled $6^1\ 2_{11}$ and $4^1\ 2_{12}$ levels, the diagonalization of the Hamiltonian including the Coriolis-coupling term yields the following expressions for the eigenfunctions:

$$\psi^{6^1}_{2_{11}} = c_1|2,1,0,1\rangle + c_2|2,-1,1,0\rangle \qquad (4)$$

$$\psi^{4^1}_{2_{12}} = c_2|2,1,0,1\rangle - c_1|2,-1,1,0\rangle \qquad (5)$$

with $|c_1|^2 = 0.9976$ and $|c_2|^2 = 0.0024$. The ratio $|c_1|^2/|c_2|^2 \approx 415$, however, exceeds by far the observed ratios of integrated intensities $I(4^1\ 2_{12})/I(6^1\ 2_{11}) \approx 5$. The reason for this discrepancy is likely to originate from the shorter predissociation lifetime of the 4^1 level compared to the 6^1 level, which reduces the probability of ionization of the 4^1 level in the $(1+1'+1^{(\prime)})$ three-photon ionization process. Saturation of the much stronger transition to the 4^1 level may also partially account for the discrepancy.

Table 3 Observed and calculated transition wave numbers of the $2^0_1 4^0_3 6^1_0$ and the $2^0_1 4^1_3$ bands of the $3p_x\ ^1A_2$–$\tilde{A}\ ^1A_2$ transition of H_2CO. The wave numbers were obtained by fitting the experimentally observed line shapes to Lorentzian profiles. The model used to calculate the line positions includes the a-type Coriolis interaction between the 4^1 and 6^1 levels of the $3p_x\ ^1A_2$ state. The root-mean-square deviation of the fit is $0.44\ cm^{-1}$, limited mainly by the large widths of the transitions (see text for additional details)

	6^1		4^1	
$^{\Delta K_a}\Delta J'_{K'_aK'_c}(J')$	$\tilde{\nu}_{obs}$	$\delta\ \tilde{\nu}^b$	$\tilde{\nu}_{obs}$	$\delta\ \tilde{\nu}^b$
$^qR_{11}(1)$	38 203.47	−0.08	38 379.99	0.10
$^qQ_{10}(1)$	38 198.77	0.33	—	—
$^qR_{10}(1)$	38 203.19	0.33	—	—
$^qP_{11}(2)$	38 193.39	−0.42	—	—
$^qQ_{11}(2)$	38 198.75	−0.38	—	—
$^qR_{11}(2)$	38 205.70	0.09	—	—
$^qP_{02}(2)$	—	—	38 370.70	0.79
$^qR_{02}(2)$	—	—	38 381.31	−0.89
$^qQ_{20}(2)$	38 199.45	−0.04	38 378.1[a]	−0.9
$^qR_{20}(2)$	38 206.90	0.03	38 386.0[a]	−0.5
$^qP_{22}(3)$	38 193.11	0.03	38 372.6[a]	0.0
$^qQ_{22}(3)$	38 200.41	−0.12	38 380.6[a]	0.5
$^qR_{22}(3)$	38 210.66	0.22	38 390.1[a]	0.0

[a] The transitions are not taken into account in the fit. [b] $\delta\tilde{\nu} = \tilde{\nu}_{obs} - \tilde{\nu}_{calc}$.

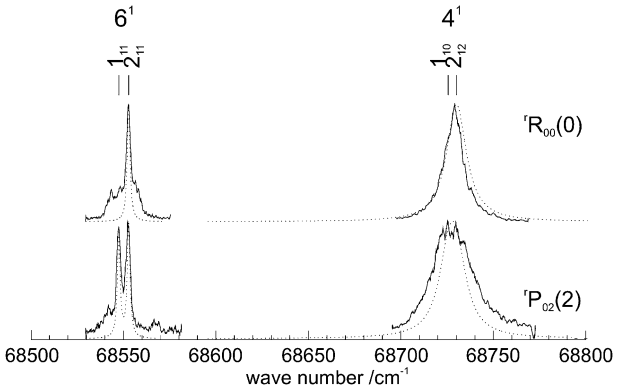

Fig. 7 Doubly-resonant three-photon ionization spectra of the 6^1 and 4^1 vibrational levels of the $3p_x\ ^1A_2$ state recorded from the $\tilde{A}\ ^1A_2\ (2^2 4^1)$ 1_{11} level. The intermediate state was reached from two different rotational levels of the $\tilde{X}\ ^1A_1$ ground state: 0_{00} (upper traces) and 2_{02} (lower traces). The dotted lines represent calculated spectra.

A similar analysis can be performed for the relative line widths (or lifetimes) of the 6^1 and 4^1 levels, using the expressions

$$\frac{1}{\tau_{6^1}} = |c_1|^2 \frac{1}{\tau^0_{6^1}} + |c_2|^2 \frac{1}{\tau^0_{4^1}} \quad (6)$$

$$\frac{1}{\tau_{4^1}} = |c_2|^2 \frac{1}{\tau^0_{6^1}} + |c_1|^2 \frac{1}{\tau^0_{4^1}}, \quad (7)$$

which relies on the assumption that only the 4^1 level is subject to predissociation. In this case, one would expect the ratios of linewidths and lifetimes to be given by

$$\frac{\Gamma_{4^1}}{\Gamma_{6^1}} = \frac{\tau_{6^1}}{\tau_{4^1}} \approx 415, \quad (8)$$

which also exceeds by far the observed ratio of linewidths (11 cm^{-1}/2.5 cm^{-1}) $\approx$ 4.5 (see Fig. 6). One must therefore conclude that the 6^1 level itself is also predissociative, though not as strongly as the 4^1 level. These results indicate that the predissociation dynamics of the $3p_x$ Rydberg state of H_2CO is complex and subtly influenced by its degree and mode of rovibrational excitation. At present, only inconclusive information on the predissociation dynamics of the 3p Rydberg states of H_2CO is available in the literature (see, for instance, ref. 13, 11) and further theoretical investigations would be extremely valuable.

Conclusions

Rotationally resolved spectra of the lowest vibrational levels of the $3p_x\,{}^1A_2$ Rydberg state of formaldehyde have been recorded by doubly-resonant three-photon ionization spectroscopy. The band origin, molecular constants and the fundamental wave numbers of the ν_4 and the ν_6 vibrational modes have been determined by analysis of several spectra obtained *via* selected rotational levels in the $\tilde{A}\,{}^1A_2$ ($2^1\,4^3$) state. A strong *a*-type Coriolis interaction between the 6^1 and the 4^1 vibrational levels has been quantified and identified as the reason for the observation of vibronically forbidden transitions to the 6^1 vibrational level. An overall good agreement of the relative intensities in the observed transitions to the 0^0 vibrational level with simulation has been found if the configuration of the polarizations of the laser beams is taken into account. The ratios of the line widths of the Coriolis-coupled levels cannot be fully accounted for by assuming that only the 4^1 level is predissociative, and a detailed theoretical study of interactions with close-lying valence and Rydberg states would be desirable.

Acknowledgements

This work was supported by the Swiss National Science Foundation (SNF) under Projects No. 200020-115958 and 200020-125030. M. M. thanks Dr M. Tulej for his assistance with preparatory experiments and Dr G. Knopp for discussions.

References

1 G. H. Dieke and G. B. Kistiakowsky, *Phys. Rev.*, 1934, **45**, 4–28.
2 D. C. Moule and A. D. Walsh, *Chem. Rev.*, 1975, **75**, 67–84.
3 D. J. Clouthier and D. A. Ramsay, *Annu. Rev. Phys. Chem.*, 1983, **34**, 31–58.
4 C. B. Moore and J. C. Weisshaar, *Annu. Rev. Phys. Chem.*, 1983, **34**, 525–555.
5 A. C. Terentis and S. H. Kable, *Chem. Phys. Lett.*, 1996, **258**, 626–632.
6 A. C. Terentis, S. E. Waugh, G. F. Metha and S. H. Kable, *J. Chem. Phys.*, 1998, **108**, 3187–3198.
7 L. R. Valachovic, M. F. Tuchler, M. Dulligan, T. Droz-Georget, M. Zyrianov, A. Kolessov, H. Reisler and C. Wittig, *J. Chem. Phys.*, 2000, **112**, 2752–2761.
8 J. M. Bowman and X. Zhang, *Phys. Chem. Chem. Phys.*, 2006, **8**, 321–332.
9 H. M. Yin, S. J. Rowling, A. Büll and S. H. Kable, *J. Chem. Phys.*, 2007, **127**, 064302.
10 M. Tulej, M. Meisinger, G. Knopp, A. M. Walser, T. Gerber and P. P. Radi, in preparation, 2009.
11 M. R. J. Hachey and F. Grein, *Can. J. Phys.*, 1995, **73**, 18–34.
12 S. D. Peyerimhoff, R. J. Buenker, W. E. Kammer and H. Hsu, *Chem. Phys. Lett.*, 1971, **8**, 129–135.
13 M. R. J. Hachey, P. J. Bruna and F. Grein, *J. Chem. Soc., Faraday Trans.*, 1994, **90**, 683–688.
14 P. J. Bruna, M. R. J. Hachey and F. Grein, *J. Phys. Chem.*, 1995, **99**, 16576–16585.
15 M. R. J. Hachey, P. J. Bruna and F. Grein, *J. Mol. Spectrosc.*, 1996, **176**, 375–384.
16 W. C. Price, *Phys. Rev.*, 1934, **46**, 529–529.
17 W. C. Price, *J. Chem. Phys.*, 1935, **3**, 256–259.
18 C. R. Lessard, D. C. Moule and S. Bell, *Chem. Phys. Lett.*, 1974, **29**, 603–605.
19 C. R. Lessard and D. C. Moule, *J. Mol. Spectrosc.*, 1976, **60**, 343–347.
20 C. R. Lessard and D. C. Moule, *J. Chem. Phys.*, 1977, **66**, 3908–3916.
21 J. B. Liu, H. T. Kim and S. L. Anderson, *J. Chem. Phys.*, 2001, **114**, 9797–9806.
22 J. E. Mentall, E. P. Gentieu, M. Krauss and D. Neumann, *J. Chem. Phys.*, 1971, **55**, 5471–5479.
23 A. M. Schulenburg, M. Meisinger, P. P. Radi and F. Merkt, *J. Mol. Spectrosc.*, 2008, **250**, 44–50.
24 R. Spence, *J. Chem. Soc.*, 1935, 338–340.
25 S. Leutwyler, Pulsed supersonic nozzle, University of Berne.
26 M. Tulej, M. Meisinger, G. Knopp, A. M. Walser, P. Beaud, T. Gerber and P. P. Radi, *J. Raman Spectrosc.*, 2006, **37**, 680–688.
27 A. Wüest, P. Rupper and F. Merkt, *Mol. Phys.*, 2001, **99**, 1941–1958.
28 C. Western, PGOPHER, a program for simulating rotational structure, University of Bristol.
29 T. Oka and Y. Morino, *J. Mol. Spectrosc.*, 1963, **11**, 349–367.
30 T. Oka, *J. Mol. Struct.*, 1995, **352**, 225–233.
31 R. N. Zare, *Angular Momentum*, John Wiley & Sons, New York, 1988.
32 P. R. Bunker and P. Jensen, *Molecular Symmetry and Spectroscopy*, NRC Research Press, Ottawa, 2nd edn, 1998.
33 T. C. Smith, C. J. Evans and D. J. Clouthier, *J. Chem. Phys.*, 2002, **118**, 1642–1648.